Transactions of the Materials Research Society of Japan 33[3] 557-560 (2008)

STRUCTURAL STUDY ON INTERFACE BETWEEN THICK GALLIUM LAYER AND SiC SUBSTRATE BY X-RAY REFLECTIVITY UNDER TRANSMISSION GEOMETRY

Takehiro Noda, Masanori Tanaka, Amane Kitahara, Tadaaki Kaneko,

Osami Sakata*, and Isao Takahashi

Faculty of Science and Technology, Kwansei Gakuin University, Sanda 6691337, Japan

*Materials Science, Japan Synchrotron Radiation Research Institute, SPring-8, Sayo 6795198, Japan

Fax: +81-795-65-9725, e-mail: z96019@kwansei.ac.jp

X-ray Reflectivity under transmission geometry (Transmitted X-ray Reflectivity (TXR)) is a promising technique which enables us to make in situ and non-destructive observation of buried interfaces. In this study, we have investigated a deeply-buried interface structure between a thick Ga layer and SiC(0001) at various temperatures with synchrotron radiation. Above 500 °C, specular TXR measured at an angle of incidence close to the critical angle for total reflection abruptly decreases. In the subsequent heating, an enhancement in diffuse scattering close to the specular TXR was observed above 1200 °C, indicating morphological variations on the interface. The TXR measurement shows that an onset temperature of atomic-scale interface evolution is unexpectedly low at the deeply buried interface between Ga and SiC.

Introduction

X-ray reflectivity (XR) is one of the widely-accepted techniques for non-destructive investigation on surface and interface structures and their morphologies. From the fitting procedures based on the dynamical scattering theory, parameters describing multi-layered structure, e.g. thickness, electron density and root mean squares of interface roughness are precisely obtained [1]. Although XR is the most effective interface-sensitive tool due to an easy control of penetration of X-rays, the application of the conventional XR to structural analysis of interfaces is often limited; for example, it would be almost impossible to get reflectivity from such an interface if the outermost layer is extraordinarily thick, i.e. a μm or more. For a very rough surface, we cannot access the buried interface, either. On the other hand, XR under transmission geometry (transmission X-ray reflectivity (TXR)) is an alternative method which overcomes the drawbacks inherent in the conventional XR mentioned above [2]. Comparison between the conventional XR and TXR is schematically shown in Fig. 1. In case of XR, X-ray impinges upon the outermost layer surface, whereas the X-ray beams escape from the outermost layer surface in TXR. The surface roughness and thickness do not affect data analysis. The key to success in TXR is a brilliant and narrow incident X-ray beam with short wavelength to reduce the absorption effect and get sufficient diffracted intensity. This is why X-rays available at third-generation synchrotron radiation facilities are suitable for the TXR method. Sufficient electron density contrast at the interface is also crucial since giving a distinct critical angle for total reflection.

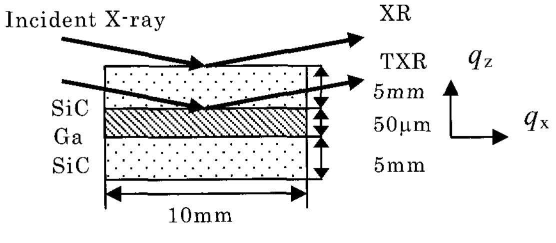

Figure 1 Side view of the sample and comparison between the XR and TXR method. Thickness of the Ga layer is exaggerated.

We investigated the deeply buried interface between Si(100) and liquid Ga and that between GaAs(100) and liquid Ga by the TXR method [3,4]. In [3], we concluded that not a few Ga atoms absorbed into the native Si oxide layer even at 150 °C. In the case of GaAs, we observed a morphological change of the interface between GaAs(100) and Ga at 250 °C [4]. Throughout these studies, we have confirmed high reactivity of thick Ga layers.

Crystal growth of SiC single crystal has been a technologically important subject. There are many reports on crystal growth by sublimation methods [5-14]. High density of micropipes and other defects including macrodefects prevent us from obtaining precise information on growth process of high quality bulk SiC crystal. An in-situ observation of SiC sublimation growth by X-ray topography has recently been performed to clarify the origin of the defect and dislocation formation [5,6]. Liquid phase growth from melt provided low-defect-density SiC bulk crystals [7-9]; however, the liquid phase epitaxy method is very difficult to grow such crystals, since SiC does not form a stoichiometric liquid phase. Quantitative studies on interfacial morphology between the melted phase and crystalline SiC are particularly valuable, although such information has been highly limited because of the lack of appropriate experimental techniques. In the present study, as a step for understanding the crystal growth of SiC in melted SiC, we investigated an interface between a thick liquid Ga layer and 4H-SiC(0001) at various temperatures by in situ TXR.

Experimental

TXR measurements were performed at beamline BL13XU at SPring-8 in which an ultra-high vacuum chamber customized for X-ray surface scattering of expitaxially grown thin films is installed [15]. The light source of BL13XU is an in-vacuum undulator which is a standard insertion device in SPring-8. The beam size was 60 μm in vertical direction and 500 μm in horizontal direction. An incident X-ray energy was tuned to be 31 keV (wavelength = 0.04 nm), that attained a 95 percent attenuation through a 10 mm thick SiC single crystal. For collecting scattered intensities, a scintillation detector was used. An ionization chamber was also used to monitor the incident X-ray; all the data were normalized using it. A sample substrate was a 5 mm thick Si-face 4H-SiC(0001) block with an area of 10 mm X 10 mm. Prior to the TXR measurement, the substrate was immersed into HF for 6 min. After the chemical cleaning, the (0001) surface morphology was examined by AFM and conventional XR. Liquid Ga was deposited onto the substrate and another SiC block with same dimension was put onto the Ga layer. In this way, we formed the sandwiched sample containing a 50 μm thick Ga layer (Fig.1). Calculated critical angle at the interface between Ga and SiC was 0.054 deg. The sample was placed in the vacuum chamber mounted on the diffractometer. The TXR data were recorded up to 1300 °C with intervals of 100 °C under a pressure better than 4 X 10^{-5} Pa. Specular TXR was obtained by the longitudinal scan (q_z-scan), whereas transverse scans (q_x-scan) were exploited to measure the off-specular TXR spectrum. After the TXR measurement in the vacuum, the Ga layer was removed from the SiC(0001) surface chemically for an ex situ re-examination by AFM.

Results

Figure 2(a) shows TXR in total reflection regime measured using the longitudinal scans. The critical angle for total reflection was experimentally determined to be 0.052 deg., which is very close to the calculated one. TXR intensity of total reflection was above 10^8 photons per sec. Figure 2(b) indicates temperature dependence of the integral intensity at q_z = 0.27 nm^{-1}, showing an abrupt decrease in intensity across 500 °C. However, the decrease in intensity becomes small with increasing the q_z values as can be seen in Fig. 2(a). Figure 3 shows the TXR profile at q_z = 1.1 nm^{-1} obtained using the transverse scans. In addition to sharp specular TXR, subsidiary diffusive enhancements in intensity, the so-called Yoneda Wings, were observed (shown in the ovals). The Yoneda Wings show maxima when the angle of incidence or the angle of exit equals the critical angle for total reflection [16]. A sudden decrease in the Yoneda Wings was observed above 500 °C.

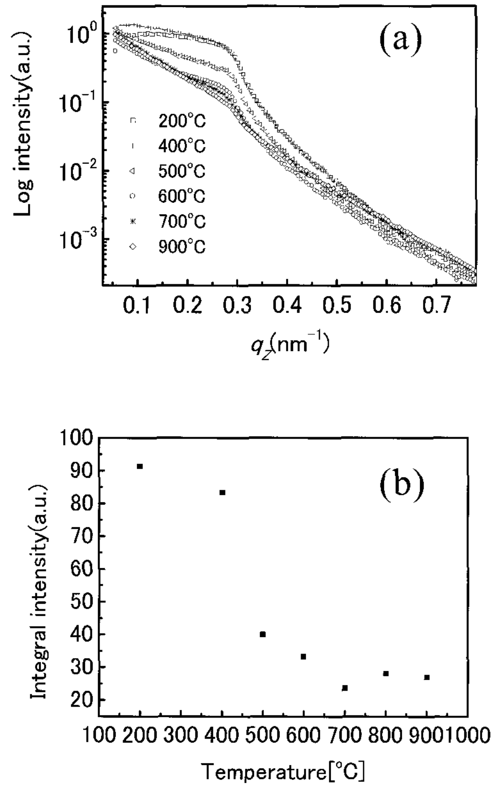

Figure 2 Longitudinal scans of TXR close to the critical angle for total reflection (a). Above 500 °C, decrease in intensity in total reflection regime (q_z<0.3 nm^{-1}) is noticed. Intensity at q_z = 0.27 nm^{-1} is plotted in (b).

Figure 4 shows temperature dependence of off-specular TXR intensity measured at $\boldsymbol{q} = (q_x, q_z) = (3.8 \times 10^{-4}$ nm^{-1}, 1.1 nm$^{-1})$ in reciprocal space, which is adjacent to the specular TXR with an incident angle of 0.18 deg. Here, the decrease in off-specular TXR intensity was also indicated around 500 °C just like in the specular TXR (Fig. 2) and also in the Yoneda Wings (Fig. 3). A sudden increase in off-specular TXR occurred above 1200 °C after the gradual increase between 500 °C and 1200 °C. After the subsequent quench from 1300 °C to room temperature, we confirmed the intensity of the off-specular TXR unchanged, indicating that the diffuse scattering above 1200 °C would not be attributed to thermal motion at the interface. We approximated the off-specular TXR at q_z = 1.1 nm^{-1} as $I_{\text{diffuse}} \sim q_x^{-\alpha}$, and fitted the exponent α, which is also indicated in Fig. 4. We can see a noticeable variation in α occurs at a temperature between 500 °C and 1200 °C, suggesting that the onset temperature for variation in surface morphology on an atomic scale is unexpectedly low, although the drastic variation in intensity is indicated above 1200 °C.

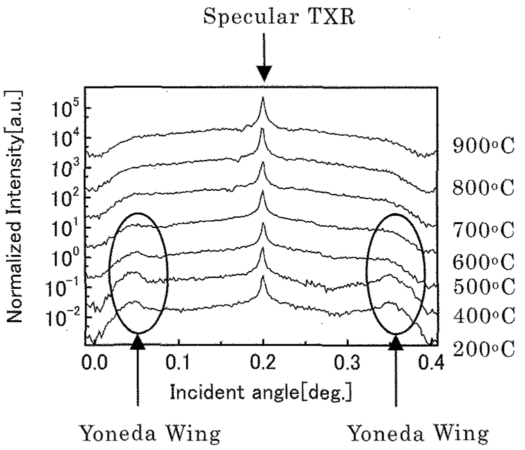

Figure 3 Yoneda Wings and specular TXR obtained by transverse scans keeping q_z = 1.1 nm^{-1}. For clarity, each data is displaced vertically.

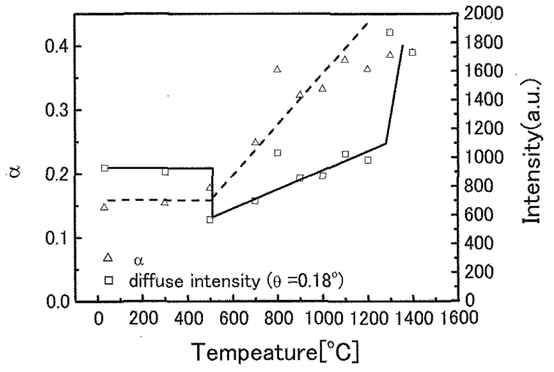

Figure 4 Temperature dependence of diffuse scattering intensity I_{diffuse} at $\boldsymbol{q} = (q_x, q_z) = (3.8\times10^{-4}$ nm^{-1}, 1.1 nm$^{-1})$ and fitted exponent α. Definition of α is $I_{\text{diffuse}} \sim q_x^{-\alpha}$. The lines are guide to eyes.

Figure 5 shows AFM images before and after the TXR measurement. Before the measurement (Fig. 5(a)), the surface looks almost flat but has many scratches due to the polishing process. After the TXR measurement (Fig. 5(b)), except for the residual contaminations on the (0001) surface, the SiC surface seems to be unchanged. From the height resolution in the present AFM, it indicates that the typical size of the morphological change shown by the present TXR study should be much less than one μm.

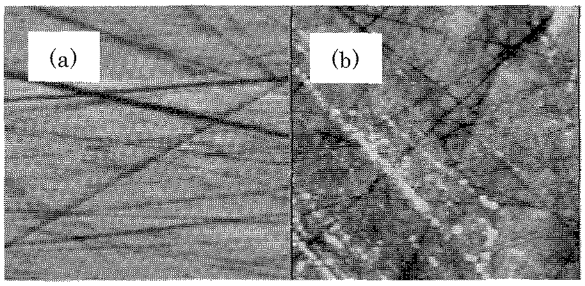

Figure 5 AFM images of the 4H-SiC (0001) surface: before TXR (a), and after TXR (b). Each image has an area of 10 μm X 10 μm.

Discussion

In Figs. 2 and 3, we have found that the sudden intensity drop around 500 °C occurs when the incident angle and/or the exit angle approaches the critical angle for total reflection. Rough interfaces usually reduce the specular XR especially with higher incident angles, which is contrary to the present result. Actually, the fitted surface roughness parameter σ which reduces XR by the factor of exp($-\sigma q_z^2$) almost unchanged throughout the TXR measurements. The obtained σ was 0.43 nm and details on all the fitted parameters will be published elsewhere. The reduction in scattered intensity with the incident (or exit) angles close to the critical angle for total reflection can be attributed to a screening effect of the incident (or exit) X-rays due to the scratches on the SiC surface which had been filled with the liquid Ga. Scratches completely filled with Ga would effectively screen and randomly scatter the incident and diffracted X-rays, since electron density of Ga is much higher than that of SiC. This screening effect would fairly be strong in the present experimental condition in which the incident and diffracted X-rays traveled in the SiC block, not in the Ga layer. Deeper scratches screen more X-rays. Assuming the number density of scratches unchanged around 500 °C, average growth of scratches on SiC(0001) around this temperature is estimated to be 1 nm in surface-normal direction, from the angular range in which the screening effect is dominant (Fig. 6). With increasing the depth of scratches, we obtain less diffracted X-rays from the (0001) interface due to the screening effect as shown in Fig. 6(b). Since the bottom of these scratches is composed of unstable planes with higher indices, nm-sized dissolubility of SiC into the liquid Ga might occurs around 500 °C. However, the stable places like (0001) terraces would hardly dissolve to the liquid Ga below 1400 °C. The results obtained by the TXR data may be supported by the AFM images which do not indicate any substantial increase in surface roughness of (0001) terraces or show apparent variation of number density of scratches. The drastic drop in intensity around 500 °C was also confirmed for the diffuse scattering as shown in Fig. 4 where the off-specular TXR eventually rises with increasing the temperature. We also observed the change of exponent α above 500 °C, which means that there was a change in parameters describing the statistical character of the interface. A complete two dimensional mapping of non-specular TXR in (q_x, q_z) plane would certainly be necessary for clarifying the change of the interface between 500 °C and 1400 °C.

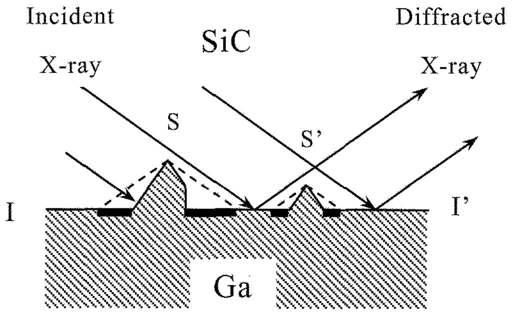

(a) below 500 ^{O}C

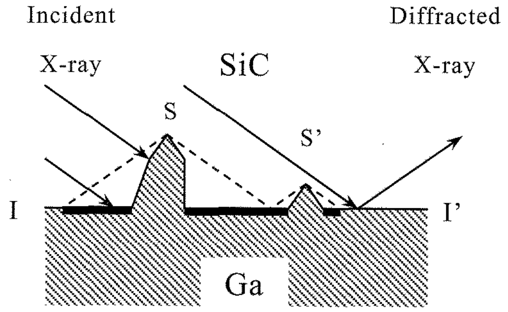

(b) above 500 ^{O}C

Figure 6 Illustrations of interface between SiC (0001) and Ga. Side views are drawn. Horizontal lines between I and I' in (a) and (b) represent the interface; the upper part of the line segment is SiC and the lower hatched part is Ga. Polygons and triangles denoted as S and S' respectively are section of scratches filled with Ga. In this study incident and diffracted X-rays travel in bulk SiC. Owing to the scratches, incident and diffracted X-rays are screened especially with extremely low incident and exit angles; the thick horizontal line segments show the screened area in Fig. 6. The deeper scratch we have (= the longer distance between the point S and the interface, as shown in (b)), the weaker TXR is obtained for low angles. In actual TXRs, the angle of incidence and exit is much smaller than the corresponding angle in this figure.

In conclusion, we confirmed the capability of TXR especially for in situ and non-destructive study on deeply buried interfaces. For the interface between SiC(0001) and liquid Ga, a subtle variation in the interface morphology presumably accompanying partial melt of SiC with 1 nm or less in depth was detected around 500 °C by several interface-sensitive X-ray scattering.

Acknowledgments

The proposal numbers of SPring-8 for the TXR measurements are 2004A0076-ND1d-np and 2004B0115-ND1d-np. SiC samples were kindly supplied by Nippon Steel Corporation Advanced Technology Research Laboratories.

References

1) L. G. Parratt: *Phys. Rev.* **95** (1954) 359-369.
2) W. J. Huisman, J. F. Peters, M. J. Zwanenburg, S. A. de Vries, T. E. Derry, D. L. Abernathy, J. F. van der Veen, *Nature* **390** (1997) 379-381.
3) I. Takahashi, K. Inoue, A. Kitahara, H. Terauchi, and O. Sakata: *Jpn. J. Appl. Phys.* **44** (2004) 1561-1565.
4) K. Inoue, A. Kitahara, K. Matsushita, H. Kikkawa, F. Nakabayashi, N. Ageishi, H. Terauchi, O. Sakata, and I. Takahashi: *Surface and Interface Analysis.* **37** (2005) 185-189.
5) H. Yamaguchi, S. Nishizawa, T. Kato. N. Oyanagi, W. Bahng, S. Yoshida, K. Arai, T. Kikuchi: *Rev. Sci. Instum.* **71** (2000) 2829-2832.
6) T. Kato, N. Oyanagi, H. Yamaguchi, S. Nishizawa, M. N. Khan, Y. Kitou, K. Arai: *J. Cryst. Growth.* **222** (2001) 579-585.
7) D. H. Hofmann, M. H. Muller: *Materials Science and Engineering.* **61/62** (1999) 29-39.
8) M. Syvajarvi, R. Yakimova, M. Tuominen, A. Kakanakova-Georgieva, M. F. MacMillan, A. Henry, Q. Wahab, E. Janzen: *J. Cryst. Growth.* **197** (1999) 147-154.
9) B. M. Epelbaum and D. Hofmann: *J. Cryst. Growth.* **225** (2001) 1-5.
10) M. Selder, L. Kadinski, F. Durst, D. Hofmann: *J. Cryst. Growth.* **226** (2001) 501-510.
11) A. S. Segal: *J. Cryst. Growth.* **208** (2000) 431-441.
12) D. Hofmann, M. Bickermann, R. Eckstein, M. Kolbl, St. G. Muller, E. Schmitt, A. Weber, A. Winnacker: *J. Cryst. Growth.* **198/199** (1999) 1005-1010.
13) T. Furusho, S. K. Lilov, S. Ohshima, S. Nishino: *J. Cryst. Growth.* **237** (2002) 1235-1238.
14) S. Yu. Karpov, Yu. N. Makarov, E. N. Mokhov, M. G. Ramm, M. S. Ramm, A. D. Roenkov, R. A. Talalaev, Yu. A. Vodakov: *J. Cryst. Growth.* **173** (1997) 408-416.
15) O. Sakata, Y. Furukawa, S. Goto, T. Mochizuki, T. Uruga, Y. Shimada, K. Takeshita, H. Ohashi, T. Ohata, T. Matsushita, S. Takahashi, and T. Ishikawa: *SPring-8 Inf.* **6** (2001) 450-455.
16) Y. Yoneda: *Phys. Rev.* **131** (1963) 2010-2013.

(Recieved December 10, 2007 ; Accepted April 25, 2008)